



# Virtual straightening of scraper conveyor based on the position and attitude solution of industrial robot model

Suhua Li<sup>1</sup> · Jiacheng Xie<sup>1</sup> · Fang Ren<sup>1</sup> · Xin Zhang<sup>1</sup> · Xuwen Wang<sup>1</sup> · Binbin Wang<sup>1</sup>

Received: 20 May 2020/Revised: 14 July 2020/Accepted: 3 December 2020/Published online: 6 February 2021  
© The Author(s) 2021

**Abstract** The movement of the floating connecting mechanism between a hydraulic support and scraper conveyor is space movement; thus, when the hydraulic support pushes the scraper conveyor, there is an error between the actual distance of the scraper conveyor and the theoretical moving distance. As a result, the scraper conveyor cannot obtain the straightness requirement. Therefore, the movement law of the floating connecting mechanism between the hydraulic support and scraper conveyor is analyzed and programmed into the Unity3D to realize accurate pushing of the scraper conveyor via hydraulic support. The Coal Seam + Equipment Joint Virtual Straightening System is established, and a straightening method based on the motion law of a floating connection is proposed as the default method of the system. In addition, a straightening simulation of the scraper conveyor was performed on a complex coal seam floor, the results demonstrate that the average straightening error of the scraper conveyor is within 2–8 mm, and is in direct proportion to the fluctuation of the coal seam floor in the strike of the seam with high accuracy, the straightness of scraper conveyor is more affected by the subsidence terrain during straightening than by the bulge terrain. And some conclusions are verified by experiment. Based on the verification of the relevant conclusions, a comparison and analysis of Longwall Automation Steering Committee (LASC) straightening technology and default straightening method in the simulation system shows that the straightness accuracy of LASC straightening technology under complex floor conditions is slightly less than that of the default straightening method in the proposed system.

**Keywords** Virtual reality · Scraper conveyor · Hydraulic support · Posture solution · Straightness control

## List of symbols

$\theta_2$	Angle of rotation of the $x_1$ axis around the $x_2$ axis	$d_1$	Distance between the $x_0$ axis and the $x_1$ axis along the $z_0$ axis
$\theta_3$	Angle of rotation of the $x_2$ axis around the $x_3$ axis	$l_1$	Distance between the $z_0$ axis and the $z_1$ axis along the $z_1$ axis
$\theta_4$	Angle of rotation of the $x_3$ axis around the $x_4$ axis	$l_2$	Distance between the $x_4$ axis and the $x_5$ axis along the $z_4$ axis
		$\hat{\theta}_i$	Angle of rotation of the $z_{i-1}$ axis about the $z_i$ axis
		${}^{i-1}T_i$	The transformation matrix of two adjacent coordinate systems
		$AFP_{n-1}$	Initial position and attitude of scraper conveyor
		$AFP_n$	Actual position and attitude of scraper conveyor after shearer cutting
		$DFP_n$	Position and attitude of scraper conveyor after straightening
		$DPC_n$	The difference between the two according to the curve of $AFP_n$ and $AFP_{n-1}$

✉ Fang Ren  
renfang@tyut.edu.cn

<sup>1</sup> Shanxi Key Laboratory of Fully Mechanized Coal Mining Equipment, College of Mechanical and Vehicle Engineering, Taiyuan University of Technology, Taiyuan 030024, China

$RPC_n$  Theoretical straightening amount of scraper conveyor

## 1 Introduction

With the emergence of intelligent manufacturing as a core technology (Wang et al. 2019; Syd et al. 2019; Meng et al. 2020; Ge et al. 2020; Wang and Huang 2017), the intelligent coal mine is the core technical support for high-quality development in the coal industry where the construction of an intelligent coal mine is the ultimate goal (Fu et al. 2017; Wang et al. 2020). However, the movement of the floating connecting mechanism of the hydraulic and the scraper conveyor is space movement; thus, an execution error and mechanical error of the hydraulic support exist (Ibrahim et al. 2011; Wang 2014). Consequently, ensuring the straightness of a fully mechanized coal mining face is difficult. With the advancement of a fully mechanized coal mining face, errors will accumulate, and such errors will affect the normal operation of the coal mine.

The straightening method of a fully mechanized coal mining face can be divided into two parts: a straightening method based on hydraulic support and a straightening method based on the scraper conveyor (Hao et al. 2017a, b). The alignment method based on hydraulic support involves installing sensors on the hydraulic support. Here the hydraulic support is taken as the fulcrum, and the straightness of the hydraulic support group is controlled to achieve the straightness control of the scraper conveyor (Li et al. 2016). Niu (2015) proposed installing a rangefinder and angle sensor on the hydraulic support to detect the alignment. The straightening method based on the scraper conveyor is primarily employed to obtain the attitude of the scraper conveyor through the track of the shearer and then straighten the scraper conveyor (Reid et al. 2011). Fang et al. (2010) proposed using inertial navigation to realize automatic positioning and attitude determination of the shearer and established a cumulative error model to improve positioning and attitude determination accuracy. Hao et al. (2017a) combined a strapdown inertial navigation device and axial encoder to obtain the operating attitude of the shearer. However, the above two straightening methods do not consider the possible unevenness of the coal floor and the space movement of the hydraulic support pushing mechanism, which will affect the straightness of the scraper conveyor.

The pushing mechanism is a floating mechanism that connects the hydraulic support and the scraper conveyor. In this paper, this mechanism is called a floating connection mechanism. When the hydraulic support pushes the scraper

conveyor, each component of the floating connecting mechanism can perform translation or rotation movement. Typically, an industrial robot is composed of several rotating joints and moving joints that are connected with each moving part in series or in parallel. This configuration can realize rotation, translation, and combined movement (Jazar 2010; Chen and Dong 2013; Fang et al. 2019; Zhang et al. 2019; Manou et al. 2019). Therefore, based on the kinematic characteristics of the floating connection mechanism between the hydraulic support and the scraper conveyor, a corresponding manipulator model can be established. After analyzing its position and posture, the result can be applied to the straightening process to achieve precise movement.

However, due to the complex environment, narrow space, and various unsafe factors, it is very difficult to carry out relevant experiments, verify conclusions, and acquire data in a coal mine. “Industry + VR” (Xie et al. 2017; Isleyen and Duzgun 2019) provides technical support for testing, research, and visualization of a comprehensive mining face under complex conditions. Unity3D is a virtual simulation engine that supports two and three dimensions using an interactive graphic development environment (Xie et al. 2019). Unity3D can not only realize the visualization of a complex working environment and establish virtual mapping of the real physical world, it can also be applied as a solver to solve complex problems and output data in real time (Xie et al. 2018a). Thus, Unity3D is well-suited to simulate an underground coal mine in Unity3D. Therefore, in view of given the existing problems existing in association with the current straightening of the scraper conveyor, the virtual straightening simulation is carried out in Unity3D, which. This approach provides a shortcut for straightening research under complex working conditions.

Given the above problems, based on an industrial robot model, this paper establishes a corresponding manipulator model according to the motion characteristics of the floating connection mechanism. The motion law of the model is analyzed and given to the hydraulic support in the form of C# in the Unity3D environment to realize cooperation between the hydraulic support and the scraper conveyor. In the Unity3D virtual simulation environment, the “Coal Seam + Equipment” Joint Virtual Straightening System is established, and a straightening method based on the motion law of the floating connection mechanism is proposed. The proposed method realizes accurate movement of the hydraulic support. By changing the relative fluctuation of the complicated cutting floor, the scraper conveyor can be straightened accurately when the electrohydraulic control error is ignored. The influence of the fluctuation of the coal seam floor on the straightness of the scraper conveyor is analyzed, and the straightening accuracy of the proposed straightening method is indirectly

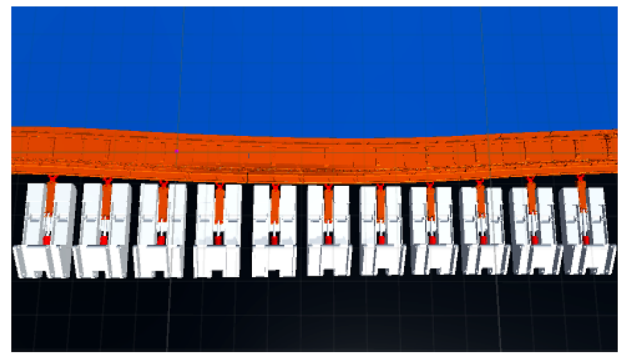
obtained. Finally, the straightening method based on the motion law of the floating connection mechanism is compared to the Longwall Automation Steering Committee (LASC) straightening technology in terms of process and accuracy.

## 2 Integral concept of virtual straightening of scraper conveyor

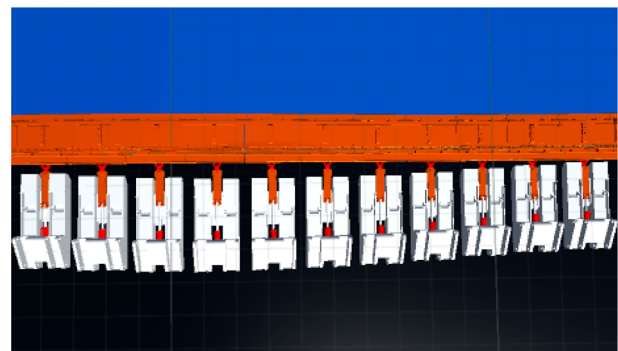
The machines involved in a fully mechanized coal mining face are hydraulic support, shearer, and scraper conveyor (Xie et al. 2017). When the working face is operational the shearer takes the scraper conveyor as the running track, cuts the coal back and forth along the coal wall, cuts the coal off the coal wall, and loads the falling coal into the scraper conveyor, which moves forward as the hydraulic support advances while carrying the coal. After the shearer completes its work, the hydraulic support supports the roof of the goaf to maintain a certain working space (Xie et al. 2018a, 2019). In the process of coal mining, the working face wall, scraper conveyor, and hydraulic support must be aligned in a straight line. However, in a fully mechanized coal mining face, the straight line requirement cannot always be met; therefore, it is necessary to straighten the scraper conveyor. The three machines in a fully mechanized coal mining face and the straightening effect are shown in Fig. 1.

The connection between the hydraulic support and the middle trough is a floating system (Wang et al. 2018; Hao et al. 2017b), as shown in Fig. 2. Thus, movement of the floating connecting mechanism of the hydraulic support and scraper conveyor is spatial rather than simple linear movement, which results in error between the moving distance of the scraper conveyor and the ideal moving distance when the scraper conveyor is pushed. Therefore, it is necessary to analyze the movement of the floating connecting mechanism between the hydraulic support and scraper conveyor.

Based on the motion law of the floating connection mechanism, the displacement of the hydraulic cylinder is obtained and straightened in the proposed “Coal Seam + Equipment” Joint Virtual Straightening System. First, the hydraulic support pushes the scraper conveyor, and the hydraulic support advances support according to elongation of the obtained hydraulic cylinder according to the position and posture of the shearer (Wang et al. 2018; Hao et al. 2017b; Liu et al. 2019). The inverted trajectory of the scraper conveyor is compared to the expected trajectory of the next knife, and straightening correction of the corresponding middle trough of the hydraulic support is obtained. Through real-time data analysis of the simulation system, the actual pushing amount of the hydraulic support



(a) State before straightening



(b) State after straightening

**Fig. 1** Three machines in fully mechanized coal face and straightening effect

corresponding to the straightening correction amount is obtained, and the hydraulic support pushes according to the pushing stroke. Finally, the running track of the scraper conveyor after straightening is obtained, and the hydraulic support moves according to extension of the hydraulic cylinder during pushing. A flowchart of the virtual straightening concept is shown in Fig. 3.

## 3 Construction of analytical model based on industrial robot

When the hydraulic support pushes the scraper conveyor, the pushing mechanism connecting the hydraulic support and scraper conveyor has four degrees of freedom, i.e., translational movement of the piston rod along the advancing ram cylinder, pitch and yaw rotation of the relay bar around the pin shaft connecting the relay bar and piston rod, and yaw rotation of the joint around the connected pin axis. Thus, the motion of the pushing mechanism is spatial movement rather than simple plane movement. Therefore, the moving mechanism is referred to as the floating connecting mechanism of the hydraulic support and scraper

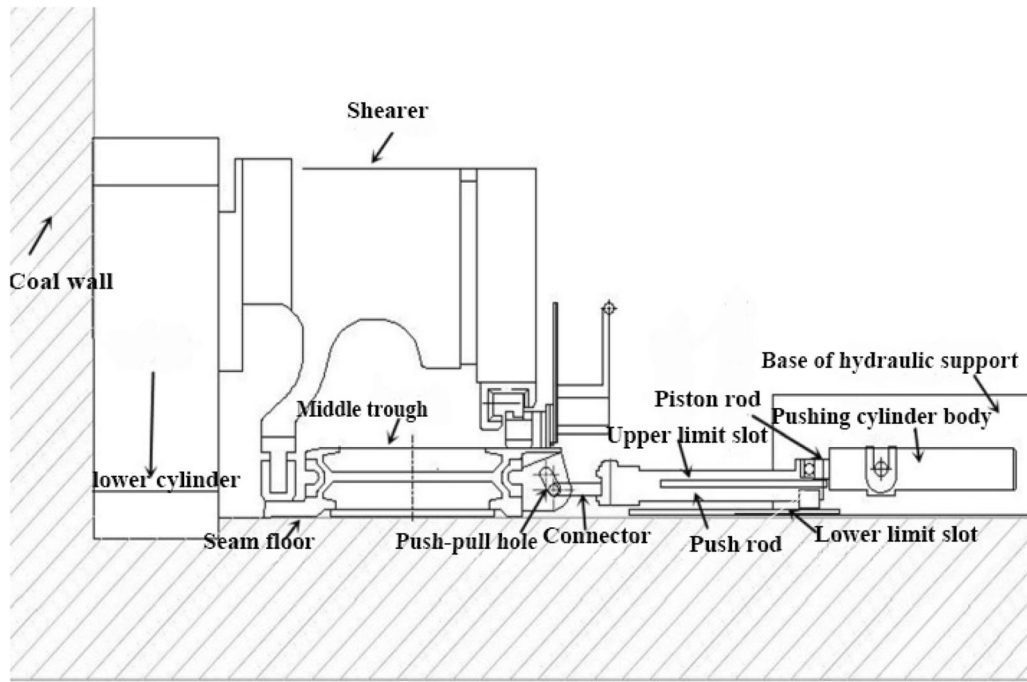


Fig. 2 Connection between hydraulic support pushing mechanism and scraper conveyor

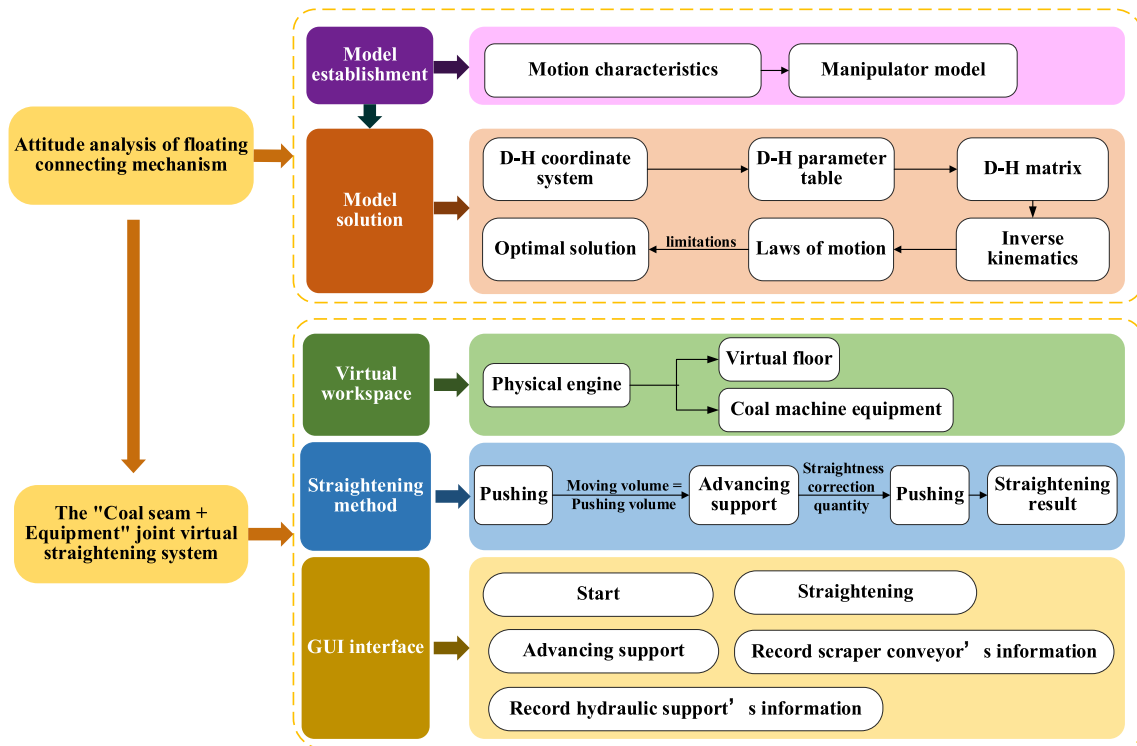


Fig. 3 Overall framework of virtual straightening of scraper conveyor

conveyor. Note that its motion characteristics are similar to those of an industrial robot.

### 3.1 Model transformation

Industrial robots comprise of a series of connecting rods connected by rotational and prismatic joints, which can locate and orient in the range of motion. Generally, the motion of connecting rods includes rotational movement, translational movement, and translational plus rotational motion (Jazar 2010). The movement of each structure of the floating connecting mechanism of the hydraulic support and scraper conveyor has rotational movement or translational movement; thus, the floating connecting mechanism can be transformed into a manipulator model.

In robot kinematics, roll, pitch, and deflection angles are used to represent the motion attitude, and the combination of angles can be used to describe the motion attitude of the robot (Manou et al. 2019). When the hydraulic support pushes the scraper conveyor, the hydraulic oil cylinder is in the static state relative to the base; therefore, the hydraulic oil cylinder is selected as the base. In addition, movement of the joint is simplified as deflection movement of the end actuator around the wrist. The joint is simplified as an end-effector, and the pin shaft connecting the joint to the relay bar is simplified as a rotating joint with yawing motion. The connecting pin between the piston rod and relay bar is simplified as a rotary joint with yawing motion and pitching motion of the robot, and the hydraulic cylinder and piston rod are simplified as the prismatic joint of the robot. The final model can realize the deflection movement of the end-effector around the wrist, the extension and retraction of the manipulator, and the pitching and deflection movement of the arm. The manipulator model is shown in Fig. 4, where Fig. 4a is a schematic diagram of the pushing mechanism, which is primarily comprises an advancing ram, relay bar, and joint, and Fig. 4b is a manipulator model obtained by converting the kinematic characteristics of each structure in Fig. 4a into corresponding joints.

### 3.2 D–H coordinate system

The D–H matrix coordinate system refers to the local reference system assigned to each joint, which must specify the  $z$ -axis and  $x$ -axis (Jazar 2010). If the joint is rotating, the  $z$ -axis is in the right-hand rotation direction, and, if the joint is translational, the  $z$ -axis is in the straight-line motion direction. Here, the  $z$ -axis of all rotating joints and prismatic joints is determined according to the above principles. When the joints are not parallel or do not intersect, the  $z$ -axis is typically a diagonal line. Note that there is always a common vertical line with the shortest distance that is

orthogonal to any two diagonal lines. The  $x$ -axis of the local coordinate system is defined in any two directions of the common vertical line. According to this method, the  $x$ -axis of all rotational and prismatic joints is determined. The D–H coordinate system shown in Fig. 5 is established according to the relative motion relationship of each joint of the determined manipulator model.

## 4 Model solving based on inverse kinematics

According to the D–H matrix coordinate system (Sect. 3.2), the linkage of the manipulator model is expressed  $P\parallel R(0^\circ), R\perp R(90^\circ), R\perp R(90^\circ), R\parallel R(0^\circ), R\perp P(90^\circ)$ . The D–H parameter table according to the established D–H matrix coordinate system is given in Table 1, and the meaning of each joint variable is listed in Table 2.

### 4.1 Solving equations by inverse kinematics

It is necessary to determine the relationship between the elongation of the piston rod, the deflection angle of the relay bar around the connecting pin shaft, the pitch angle and the deflection angle of the joint.

Equation (1) shows the transformation matrix of two adjacent coordinate systems.

$${}^{i-1}T_i = \begin{bmatrix} \cos \theta_i & -\sin \theta_i \cos \alpha_i & \sin \theta_i \sin \alpha_i & a_i \cos \theta_i \\ \sin \theta_i & \cos \theta_i \cos \alpha_i & -\cos \theta_i \sin \alpha_i & a_i \sin \theta_i \\ 0 & \sin \alpha_i & \cos \alpha_i & d_i \\ 0 & 0 & 0 & 1 \end{bmatrix} \quad (1)$$

All transformation matrices of the manipulator model are obtained as follows.

$${}^0T_1 = \begin{bmatrix} 1 & 0 & 0 & 0 \\ 0 & 1 & 0 & 0 \\ 0 & 0 & 1 & d_1 \\ 0 & 0 & 0 & 1 \end{bmatrix} \quad (2)$$

$${}^1T_2 = \begin{bmatrix} \cos \theta_2 & 0 & \sin \theta_2 & 0 \\ \sin \theta_2 & 0 & -\cos \theta_2 & 0 \\ 0 & 1 & 0 & 0 \\ 0 & 0 & 0 & 1 \end{bmatrix} \quad (3)$$

$${}^2T_3 = \begin{bmatrix} \cos \theta_3 & 0 & \sin \theta_3 & 0 \\ \sin \theta_3 & 0 & -\cos \theta_3 & 0 \\ 0 & 1 & 0 & 0 \\ 0 & 0 & 0 & 1 \end{bmatrix} \quad (4)$$

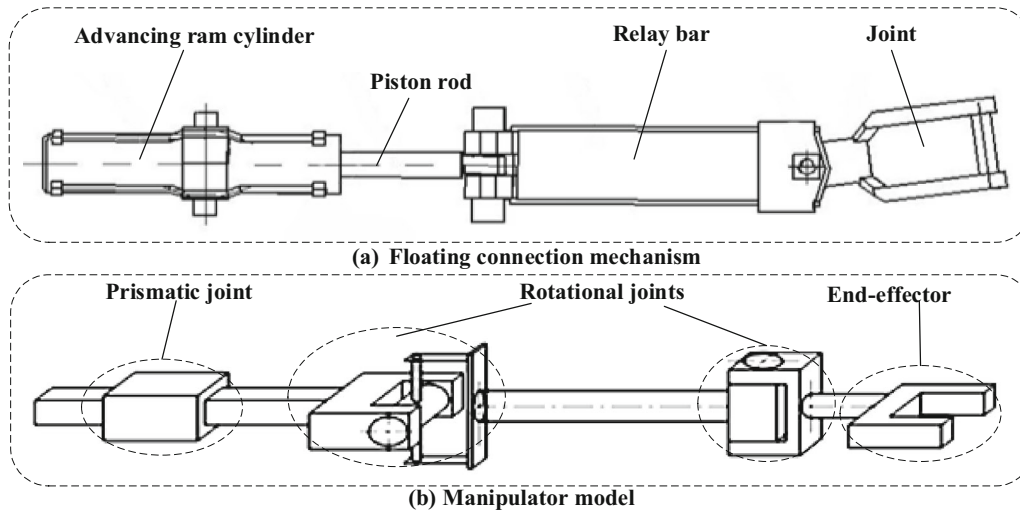


Fig. 4 Hydraulic support floating connection mechanism and conversion model

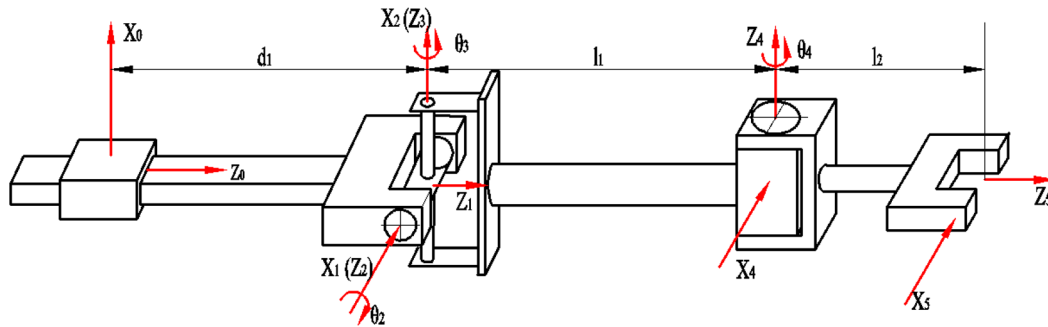


Fig. 5 D-H reference frame

Table 1 D-H parameters

Joint serial number	$\theta_i$	$d_i$	$a_i$	$\hat{\sigma}_i$ (°)
1	0	$d_1$	0	0
2	$\theta_2$	0	0	90
3	$\theta_3$	0	0	90
4	$\theta_4$	0	$l_1$	0
5	0	$l_2$	0	0

$${}^3T_4 = \begin{bmatrix} \cos \theta_4 & \sin \theta_4 & 0 & l_1 \cos \theta_4 \\ \sin \theta_4 & -\cos \theta_4 & 0 & l_1 \sin \theta_4 \\ 0 & 0 & 1 & 0 \\ 0 & 0 & 0 & 1 \end{bmatrix} \tag{5}$$

$${}^4T_5 = \begin{bmatrix} 1 & 0 & 0 & 0 \\ 0 & 1 & 0 & 0 \\ 0 & 0 & 1 & l_2 \\ 0 & 0 & 0 & 1 \end{bmatrix} \tag{6}$$

Table 2 Definition of joint variables

Joint variable	Definition
Joint angle ( $\theta_i$ )	The angle of rotation of the $x_{i-1}$ axis around the $x_i$ axis
Joint distance ( $d_i$ )	The distance between the $x_{i-1}$ axis and the $x_i$ axis along the $z_{i-1}$ axis
linkage length ( $a_i$ )	The distance between the $z_{i-1}$ axis and the $z_i$ axis along the $z_i$ axis
Twist angle of connecting rod ( $\hat{\sigma}_i$ )	The angle of rotation of the $z_{i-1}$ axis about the $z_i$ axis



According to the equation  ${}^0T_5 = {}^0T_1 \cdot {}^1T_2 \cdot {}^2T_3 \cdot {}^3T_4 \cdot {}^4T_5$ , the forward motion matrix of the manipulator model is established as follows.

$${}^0T_5 = \begin{bmatrix} r_{11} & r_{12} & r_{13} & r_{14} \\ r_{21} & r_{22} & r_{23} & r_{24} \\ r_{31} & r_{32} & r_{33} & r_{34} \\ 0 & 0 & 0 & 1 \end{bmatrix} \tag{7}$$

The symbols in the Eq. (7) are as follows:

$$\begin{aligned} r_{11} &= \cos \theta_2 \cos \theta_3 \cos \theta_4 + \sin \theta_2 \sin \theta_4 \\ r_{12} &= -\cos \theta_2 \cos \theta_3 \sin \theta_4 + \sin \theta_2 \cos \theta_4 \\ r_{13} &= \cos \theta_2 \sin \theta_3 l_2 \cos \theta_2 \sin \theta_3 \\ &\quad + l_1 (\cos \theta_2 \cos \theta_3 \cos \theta_4 + \sin \theta_2 \sin \theta_4) \\ r_{21} &= \sin \theta_2 \cos \theta_3 \cos \theta_4 - \cos \theta_2 \sin \theta_4 \\ r_{22} &= -\sin \theta_2 \cos \theta_3 \sin \theta_4 - \cos \theta_2 \cos \theta_4 \\ r_{23} &= \sin \theta_2 \sin \theta_3 \\ r_{31} &= \sin \theta_3 \cos \theta_4 \\ r_{32} &= -\sin \theta_3 \sin \theta_4 \\ r_{33} &= -\cos \theta_3 \\ r_{34} &= -l_2 \cos \theta_3 + l_1 \sin \theta_3 \cos \theta_4 + d_1 \end{aligned}$$

When the end position vectors are  $(x_0, y_0, z_0)$ , the forward motion matrix is simplified as follows.

$${}^0T_5 = \begin{bmatrix} r_{11} & r_{12} & r_{13} & x_0 \\ r_{21} & r_{22} & r_{23} & y_0 \\ r_{31} & r_{32} & r_{33} & z_0 \\ 0 & 0 & 0 & 1 \end{bmatrix} \tag{8}$$

The inverse kinematics technique is used to solve the motion parameters according to the following equation.

$${}^1T_5 = {}^0T_1^{-1} \cdot {}^0T_5 \tag{9}$$

$${}^2T_5 = {}^1T_2^{-1} \cdot {}^0T_1^{-1} \cdot {}^0T_5 \tag{10}$$

$${}^3T_5 = {}^2T_3^{-1} \cdot {}^1T_2^{-1} \cdot {}^0T_1^{-1} \cdot {}^0T_5 \tag{11}$$

$${}^4T_5 = {}^3T_4^{-1} \cdot {}^2T_3^{-1} \cdot {}^1T_2^{-1} \cdot {}^0T_1^{-1} \cdot {}^0T_5 \tag{12}$$

$$I = {}^4T_5^{-1} \cdot {}^3T_4^{-1} \cdot {}^2T_3^{-1} \cdot {}^1T_2^{-1} \cdot {}^0T_1^{-1} \cdot {}^0T_5 \tag{13}$$

### 4.2 Determining the optimal solution

Due to the multi-solution problem in inverse kinematics, it is necessary to determine the optimal solution. However, movement of the floating connection mechanism between the hydraulic support and scraper conveyor is a four degree-of-freedom space motion, and the motion of each degree of freedom is random. Unity3D, as a virtual simulation engine, can assign motion laws to a specified model to control its motion.

We assign the obtained motion law to the virtual hydraulic support and mark the key point in the scraper

conveyor pushing an ear socket as the final position of the end actuator of the manipulator model. As the posture of the virtual scraper conveyor changes with the advancing virtual comprehensive mining face, the positions of the key points change in real time in the virtual environment. In addition, the points of action when pushing and advancing the support are determined by changing the positions of key points on the scraper conveyor. In the C# programming language environment, the joint variable  $d_1$  is defined as Position,  $\theta_2$  as ZhuanJiao2,  $\theta_3$  as ZhuanJiao3, and  $\theta_4$  as ZhuanJiao4. The optimal solution for different conditions is transformed into the C# language, and the movement and rotation of the related structure of the virtual floating linkage are controlled by Position, ZhuanJiao2, ZhuanJiao3, and ZhuanJiao4. The optimal solution can be determined according to the yaw and pitch angles of the relay bar around the connecting pin axis and whether the relay bar and joint interfere with the base of the hydraulic support and push ear seat of the scraper conveyor.

$$d_1 = z_0 - \sqrt{(l_1 + l_2)^2 - (x_0^2 + y_0^2)} \tag{14}$$

$$\theta_2 = \tan^{-1} \frac{x_0}{y_0} \tag{15}$$

$$\begin{aligned} \theta_3 &= \sin^{-1} \frac{l_2}{\sqrt{(x_0 \cos \theta_3 + y_0 \sin \theta_3)^2 + (z_0 - d_1)^2}} \\ &\quad + \cos^{-1} \frac{z_0 - d_1}{\sqrt{(x_0 \cos \theta_3 + y_0 \sin \theta_3)^2 + (z_0 - d_1)^2}} \end{aligned} \tag{16}$$

$$\begin{aligned} \theta_4 &= \cos^{-1} \frac{x_0 - l_2 \cos \theta_2 \cos \theta_3}{\sqrt{(l_1 \cos \theta_2 \cos \theta_3)^2 + (l_1 \sin \theta_3)^2}} \\ &\quad + \cos^{-1} \frac{l_1 \cos \theta_2 \cos \theta_3}{\sqrt{(l_1 \cos \theta_2 \cos \theta_3)^2 + (l_1 \sin \theta_3)^2}} \end{aligned} \tag{17}$$

As shown in Fig. 6, after determining the position of the pushing and advancing points, the floating connecting mechanism reaches the appropriate position. In addition, by comparing the attitude of the floating connecting mechanism in the virtual environment to that in the virtual environment, we find that the attitude motion of the floating connecting mechanism in the virtual environment is the same as that in the actual environment, and the joint and relay bar are deflected, which demonstrates that the selected motion law is reasonable.

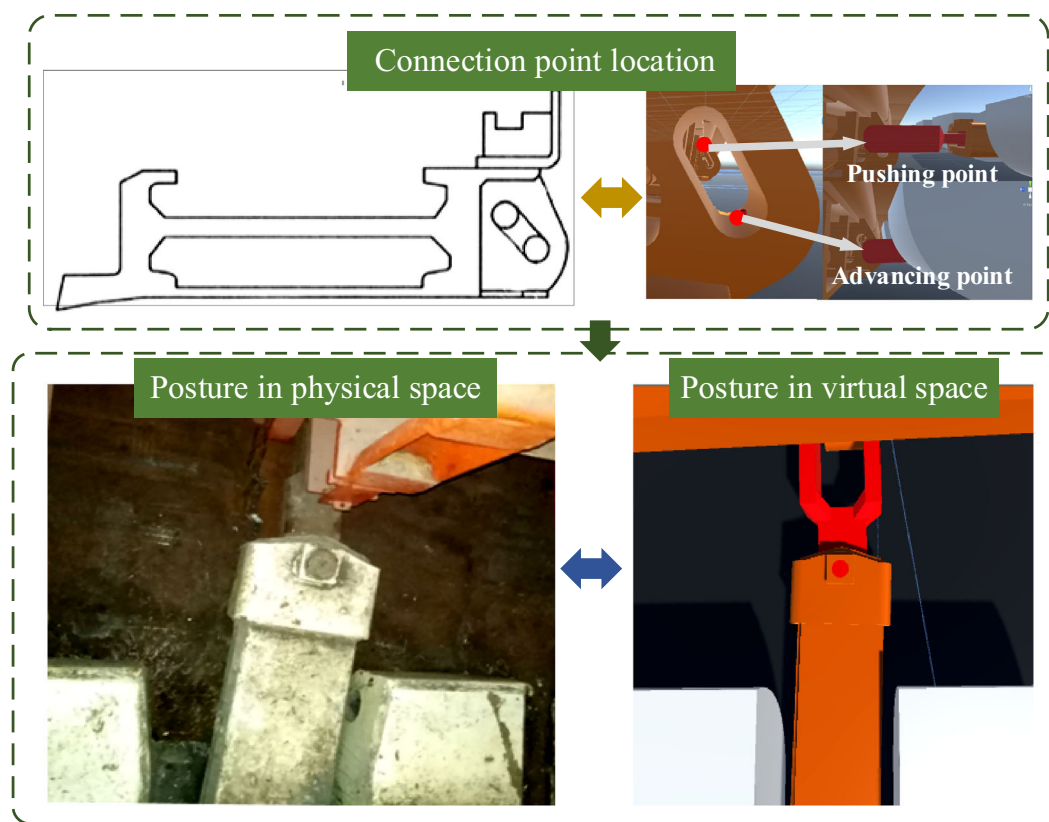


**Fig. 6** Connection diagram of hydraulic support and scraper conveyor

## 5 “Coal Seam + Equipment” joint virtual straightening system

Here, we establish the “Coal Seam + Equipment” Joint Virtual Straightening System, discuss the “Coal Seam + Equipment” Joint Virtual Straightening System, and present the virtual space of the straightening simulation. Here, to achieve coordination between the hydraulic support and scraper conveyor, the scraper conveyor can be adjusted by controlling the fluctuation of the coal floor in the direction of advance of a fully mechanized coal mining face and by means of the straightening method based on the motion law of the floating connection mechanism (Xie et al. 2018b, c, d; Shi et al. 2019).

### 5.1 Construction of “Coal Seam + Equipment” virtual scene

Large fluctuation of the coal seam floor will occur due to the influence of an uneven basement and late geological tectonic movement during coal seam deposition (Wu 2013). In addition, crustal movement will change, steepen, or slow the previously horizontal coal seam (Li 2019). In this paper, the inclination of the coal seam is 10 degrees,

and there are fluctuations in the direction of the fully mechanized coal mining face.

A three-dimensional model of the virtual coal seam floor with 10 degree inclination and undulations is built in UG, imported into 3D Max in STL format, and then converted to FBX format and imported into Unity 3D to obtain the coal seam floor in a virtual environment (Fig. 7).

Here, to simplify the research process, 11 hydraulic supports and 13 middle troughs are selected. In the virtual environment created using Unity 3D, a mesh collider is added to the virtual coal seam (Fig. 6), a box collider and rigid body components are installed on the virtual scraper conveyor and virtual hydraulic support, and a capsule collider is installed at the middle trough ramp plate of each section of the scraper conveyor to allow it to pass over raised terrain. Installing character joint hinges between the two adjacent middle troughs enables a single midsection slot to be constrained by the two adjacent middle troughs and correspond to real-world physical effects by setting parameters, i.e., the hydraulic support and scraper conveyor can be adapted to lay on the virtual coal seam (Fig. 8). Here, when the hydraulic support pushes the scraper conveyor, the middle trough is influenced by the adjacent middle trough and coal seam floor.



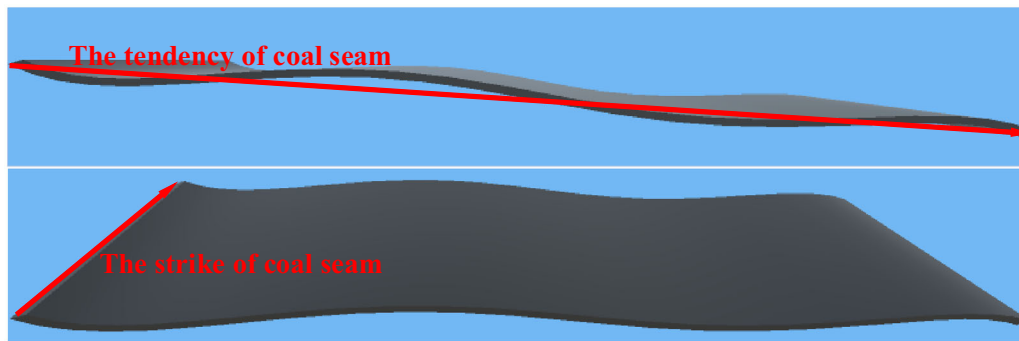


Fig. 7 Virtual coal seam

## 5.2 Establishing “Coal seam + Equipment” control model

The hydraulic support is numbered DiZuo  $X$  ( $X \in (1,11)$ ) and is considered the sub-object of  $yyzz$ . The middle trough is numbered ZhongBuCao  $X$  ( $X \in (1,13)$ ) and considered a sub-object of GBJ. The undulations along the working face direction are indicated by the relative position relationship of the two undulating coal seam floor plates, which are numbered MeiCengDiBan  $X$  ( $X \in (1,2)$ ).

According to the known running track of the shearer, the projected track in the horizontal direction is inverted to the scraper conveyor according to the bending condition of the track. Then, the bending angle of the middle trough of each section is determined and represented by the script form of GBJControl.cs, which is installed on the parent object GBJ of the middle trough of the scraper conveyor. The rotation of the middle trough of each section is controlled by the following function:

```
this.transform.Rotate(new Vector3(eulerAngles.x,
eulerAngles.y, eulerAngles.z), Space.Self);
```

The YYZJControl.cs control script is installed on each hydraulic support, and the pushing and advancing support processes of the hydraulic support is controlled by TuiYiYouGangShenChangFunction and DiZuoQianYiFunction, respectively. According to the obtained motion law of the floating connection mechanism,

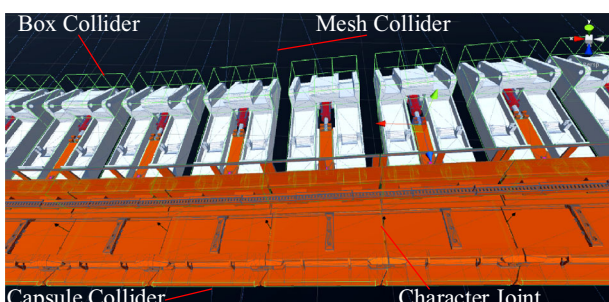


Fig. 8 “Coal seam + Equipment” based on Virtual Engine

joint variable  $d_1$  is defined as Position,  $\theta_2$  as ZhuanJiao2,  $\theta_3$  as ZhuanJiao3, and  $\theta_4$  as ZhuanJiao4. The optimal solution established under different conditions is converted to the C# language, and the movement and rotation of the relevant structures of the virtual floating connection mechanism are controlled by Position, ZhuanJiao2, ZhuanJiao3, and ZhuanJiao4 to realize precise shift of the hydraulic support.

The MCDDBControl.cs control script is installed on MeiCengDiBan1 to control the movement of MeiCengDiBan2 relative to the parent object Using the following statement: `this.transform.localPosition = new Vector3(x, y, z)`.

## 5.3 Straightening method based on motion law of floating connection mechanism

The straightening method based on the motion law of the floating connection mechanism realizes straightening of the scraper conveyor in the virtual environment, which is based on the ideal straightening position of the scraper conveyor. The hydraulic support pushing mechanism can accurately push the specific motion according to the results of each structure of the motion law of the floating connection mechanism. The law is considered the default straightening method in the “Coal Seam + Equipment” joint virtual straightening system.

The motion law of the floating connection mechanism between the hydraulic support and scraper conveyor (Sect. 4.2) is programmed into the background program of the virtual simulation system, and the virtual hydraulic support is connected to the virtual scraper conveyor by the pushing mechanism. As a result, self-adaptive collaborative propulsion of the virtual hydraulic support and virtual scraper conveyor under different coal seam conditions is realized.

As shown in Fig. 9, propelling deviation during the propelling process of the fully mechanized coal face is shown in Fig. 9. Here,  $AFP_n$  is the actual track of the working face at the cutting time of the knife  $n$ ,  $DFP_n$  is the

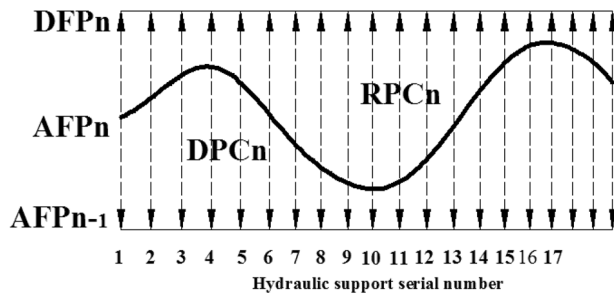


**Fig. 9** Deviation degree of advance in the process of working face advance

target trajectory of the working surface at the time of knife  $n$  cutting,  $RPC_n$  is the straightness correction required by the scraper conveyor after knife  $n$  cutting (Fan et al. 2012; Li 2019), and  $DPC_n$  is the theoretical traveling distance required for the hydraulic support after knife  $n$  has been cut. Note that the maximum values of  $RPC_n$  and  $DPC_n$  are 630 mm.

After the shearer cutting, the scraper conveyor is pushed by the hydraulic support according to the traditional process, and the  $AFP_n$  curve is obtained only after shearer cutting is completed. The simulation system obtains  $DPC_n$  according to the prediction of  $AFP_{n-1}$  and calculates the difference between the two according to the curve of  $AFP_n$  and  $AFP_{n-1}$ . In other words,  $DPC_n$  is the basis of the hydraulic support's travel, and the hydraulic support is moved according to the actual elongation of the piston rod corresponding to the calculated difference. During the next cut of coal by the shearer, the simulation system calculates the difference between the  $AFP_n$  and  $DFP_n$  curves; thus,  $RPC_n$  is the theoretical basis of this pushing stroke of the hydraulic support. After the system calculates the actual pushing stroke and sends it to the hydraulic support, the hydraulic support group pushes the scraper conveyor into a straight line on the horizontal projection. Finally, the hydraulic support is advanced according to the elongation of the piston rod. After the support is advanced, the position of the hydraulic support is adjusted, and the hydraulic support is set in position.

#### 5.4 Virtual simulation process based on seam floor without undulations

In this paper, the hydraulic support model is ZY11000/18/38D, the shearer model is MG400/920-WD, the scraper conveyor model is SGZ800/1050. In the virtual environment, the three machines of a virtual fully mechanized coal mining face are the same as those of a real fully mechanized coal mining face (with a shearer cut depth of 630 mm).

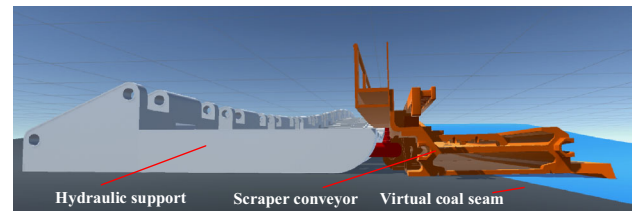


**Fig. 10** Hydraulic support group and scraper conveyor are laid on virtual coal seam

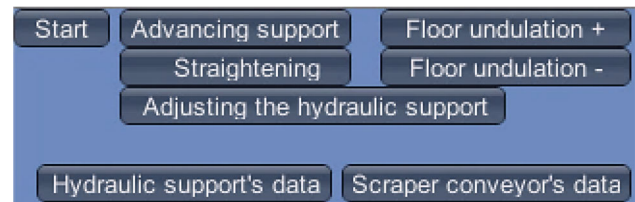


**Fig. 11** Operation interface

Since the theoretical displacement is based on the relative position change of the scraper conveyor when straightening, here, the movement of the hydraulic support is controlled by the position change of the scraper conveyor. In the virtual environment, Unity3D as a solver is used to simulate the function of the control host through the control of C# script to realize collaborative control of the hydraulic support and scraper conveyor (Li 2019).

When the virtual seam floor does not fluctuate in the direction of a fully mechanized coal mining face, the hydraulic support groups and scraper conveyors are laid on the virtual seam adaptively, as shown in Fig. 10, where the blue plate is the child plate, and the black plate is the parent plate. Here, fluctuation is indicated by changing the relative displacement of the child plate relative to the parent plate in the  $y$ -axis direction.

##### 5.4.1 Operation process

The operation interface of The “Coal Seam + Equipment” Joint Virtual Straightening System is shown in Fig. 11.

By clicking the “Start” button, the hydraulic support pushes the scraper conveyor. At this time, the scraper conveyor bends into the established posture. In addition, by clicking the “Advancing support” button, the hydraulic support group advances, and, by clicking on the “Straightening” button, the hydraulic support slides according to the forecasted track of the previous scraper conveyor. By clicking the “Advancing support” button again, the hydraulic support is advanced. Note that, at this time, the hydraulic support group does not meet the straightness requirements. Clicking the “Adjusting the hydraulic support” button adjusts the straightness of the

hydraulic support group by adjusting the position of the hydraulic support. The entire straightening process is shown in Fig. 12. Here, the hydraulic support is straightened based on the straightening method of the motion law of the floating connection mechanism, and then the hydraulic support position is straightened according to the sequence of pushing and then advancing. As can be seen, the final posture of the scraper conveyor and hydraulic support has good straightness.

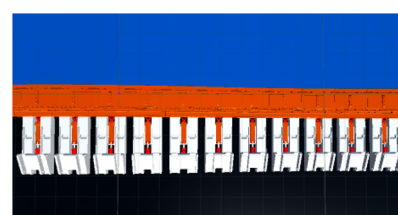
By clicking the “Hydraulic support’s data” button, data of the elongation of the piston rod, deflection angle of the joint, deflection angle of the relay bar, and pitch angle of the hydraulic support group can be output in real time in XML format during operation of the three machines of a fully mechanized virtual coal mining face. Here, the key point is marked as the position of the middle trough at the center of the middle pin row of the middle trough. By clicking the “Scraper Conveyor’s Data” button, the position of each middle trough of the scraper conveyor is output in XML file format in real time.

By clicking “Floor undulation+,” trigger once to achieve a floor bulge of 20 mm. In the simulation system, the difference between the sub-floor and the parent floor is + 0.01 dm. Click on “Floor undulations -,” trigger once to achieve a floor sag of 20 mm, in the simulation system, the difference between the sub-floor and the parent floor is – 0.01 dm.

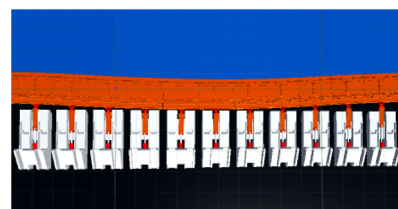
#### 5.4.2 Simulation results

Output the position coordinates of each middle trough, and the Z coordinate is selected to obtain the position curve of the scraper conveyor track projected in the horizontal direction. According to the change of the relative position of the middle trough, no more than one cutting depth can be predicted to predict the position of the scraper conveyor after straightening. Here, the average z-axis value of all middle troughs after straightening is selected as the ideal straightening position of each middle trough of the scraper conveyor.

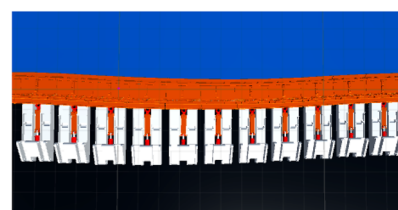
The position and posture track of the scraper conveyor in the horizontal projection direction is shown in Fig. 13a, which shows that the effect of the proposed straightening method meets the requirements of straightening. Figure 13b shows that the error between the actual and ideal track curves of the scraper conveyor is within  $\pm 0.05$  dm, and the straightening accuracy is high.



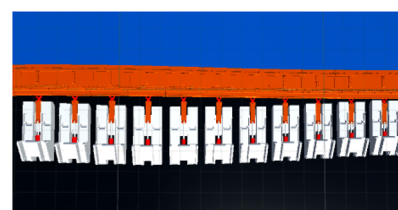
(a) Initial state



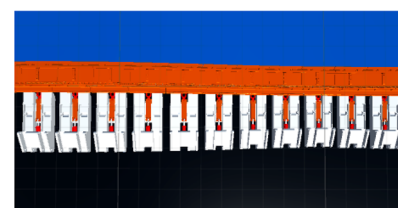
(b) After pushing



(c) After advancing support



(d) Straightening

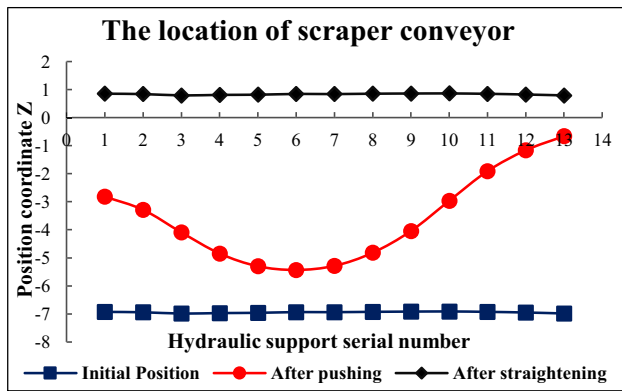


(e) Advancing support

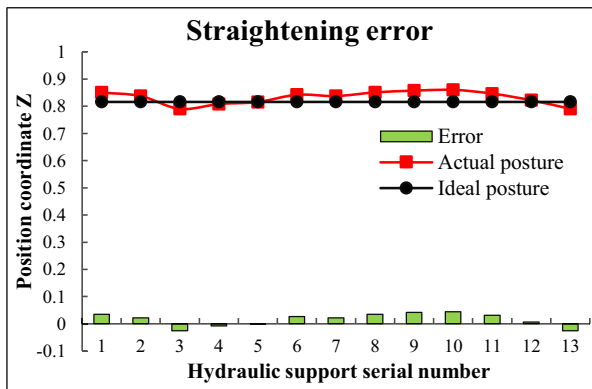


(f) Adjusting the hydraulic supports

Fig. 12 Virtual straightening process



(a) The location of scraper conveyor



(b) Straightening error

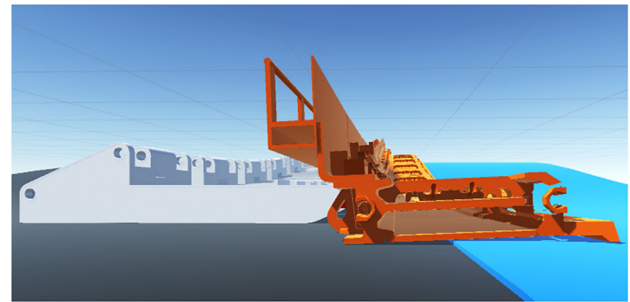
Fig. 13 Position and straightening error of Scraper conveyor

## 6 Virtual simulation test under different coal seam floor fluctuation conditions

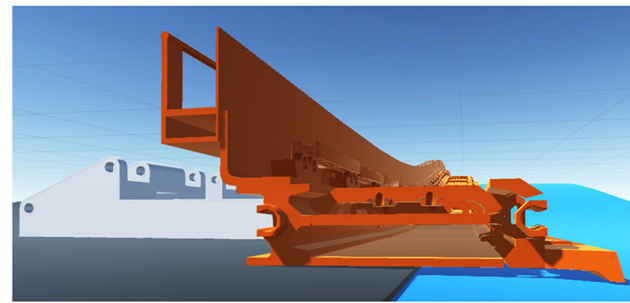
Note that the coal floor is not straight; thus, coal seam inclination and fluctuation in the direction of the fully mechanized coal mining face will occur. Here, fluctuation of the coal seam floor in the direction of the fully mechanized coal mining face is indicated by the change in the relative position between the subfloor and parent floor. As shown in Fig. 14, when the coordinate position of the sub-base plate relative to the parent base plate changes to a positive value, the terrain shown in Fig. 14a is obtained. In addition, when the coordinate position of the sub-base plate relative to the parent base plate changes to a negative value, the terrain shown in Fig. 14b is obtained.

### 6.1 Bulge topography in coal seam floor

The influence of protruding terrain on straightening accuracy when the scraper conveyor encounters raised terrain during straightening was examined in several sets of experiments. The results are shown in Table 3.



(a) The convex terrain



(b) The subsidence terrain

Fig. 14 Undulation of coal seam floor in working face

According to the Table 3, the virtual straightening simulation tests were performed using Unity3D and the straightness error of the middle trough of the scraper conveyor after straightening in the horizontal projection direction was obtained (Table 4). As can be seen, with increasing coal seam floor bulge, the average straightness error of scraper conveyor was within 3–5 mm, and the straightening accuracy was high.

By controlling coal floor bulge in the direction of advance of a fully mechanized coal mining face within the range shown in Table 4, Fig. 15a shows that, with fluctuation of the coal seam floor, a greater bulge in the coal seam floor yields greater straightening error. In addition, Fig. 15b shows that the average straightening error of the scraper conveyor increases with increasing coal seam floor bulge, when the bulge is greater than 80 mm, the average straightening error of scraper conveyor is affected more by fluctuation of the floor.

### 6.2 Subsidence topography in coal seam floor

Table 5 shows the influence of raised terrain on straightening accuracy when the scraper conveyor encounters sagging terrain while straightening.

According to the Table 5, the virtual straightening simulation tests were performed in Unity3D, and the



**Table 3** Test arrangements

Test serial number	Limits of simulation conditions (Other parameters are consistent)
1	The uplift of coal seam floor in the direction of advance of fully mechanized mining face is 20 mm
2	The uplift of coal seam floor in the direction of advance of fully mechanized mining face is 40 mm
3	The uplift of coal seam floor in the direction of advance of fully mechanized mining face is 60 mm
4	The uplift of coal seam floor in the direction of advance of fully mechanized mining face is 80 mm
5	The uplift of coal seam floor in the direction of advance of fully mechanized mining face is 100 mm

**Table 4** Straightness error of the scraper conveyor with different base plate protrusions

Test serial number	Fluctuation of coal seam floor (mm)	Straightness error (mm)		
		Maximum error	Minimum error	Average error
1	20	7.4	0.01	3.81
2	40	8.1	0.5	4.15
3	60	8.6	0.4	4.318
4	80	8.4	1.4	4.32
5	100	9.8	0.03	4.88

straightness error of the middle trough of the scraper conveyor after straightening in the horizontal projection direction was obtained. The results are shown in Table 6. As can be seen, with increasing coal seam floor subsidence, the average straightness error of scraper conveyor was within 2–8 mm, and the straightening accuracy is high.

By controlling the subsidence of the coal floor in the direction of the working face advance in the range of fluctuation of coal floor (Table 6). Figure 16a shows that, with coal seam floor fluctuation, larger subsidence of the coal seam floor results in greater straightening error of the scraper conveyor. In addition, Fig. 16b shows that the average straightening error of the scraper conveyor increases as subsidence of the coal seam floor increases. Here, the average straightening error of the scraper conveyor is increasingly affected by floor fluctuation.

### 6.3 Test conclusions

- (1) From the simulation results presented in Sects. 6.1 and 6.2, it can be seen that, in the virtual environment, the straightening method based on motion law of floating connection mechanism is used to straighten the alignment. The straightening effect is better, and the straightening precision is high.
- (2) When the coal seam floor fluctuates in the advancing direction of a fully mechanized coal mining face, the scraper conveyor straightness error increases after straightening.
- (3) When the coal seam floor in the fully mechanized coal face has undulations, the straightness of scraper conveyor is more affected by the subsidence terrain

during straightening than by the bulge terrain. However, when the bulge is within 20–100 mm, the average straightness error of the scraper conveyor after straightening is within 4–5 mm. When the subsidence is within 20–100 mm, the average scraper conveyor straightness error after straightening is within 2–8 mm. And the two cases have high straightening accuracy and meet the accuracy requirements of straightening.

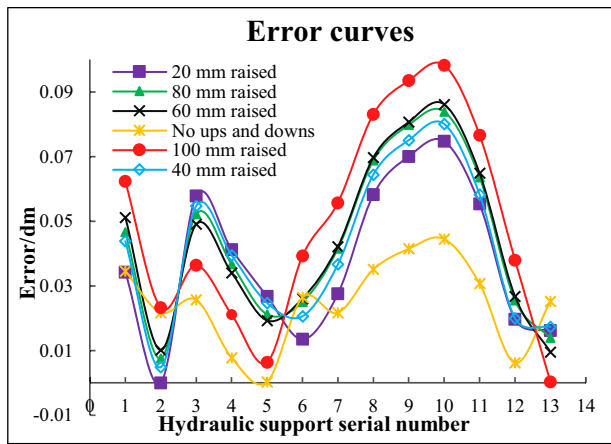
## 7 Experimental verification

### 7.1 Experimental scheme and platform

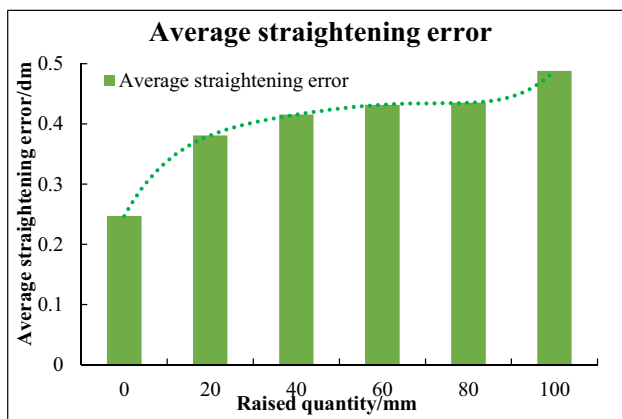
According to the scale between the pushing test-bed model and the coal machinery model in the virtual simulation system is about 6:35. According to the median line of triangle, 3.5 mm gaskets are selected to control the fluctuation of the base plate, the fluctuating model of coal seam floor is shown in Fig. 17.

The sensors required in this paper are listed in Table 7, and the experimental device is shown in Fig. 18. Due to the limitation of the experimental device, the angle of the joint is obtained by manual measurement. And the test-bed is fixed on the foundation, it cannot realize the advancing of the base, so the pushing mechanism can only push the scraper conveyor with full stroke to control the straightness of the scraper conveyor. In this experiment, by controlling the undulations of the coal floor model, the board is made to walk along the white line on the middle trough to





(a) Error curves



(b) Average straightening error

Fig. 15 Straightening error of coal seam floor when there is bulge in its advancing direction

Table 5 Test arrangements

Test serial number	Limits of simulation conditions (other parameters are consistent)
1	The subsidence of coal seam floor in the direction of advance of fully mechanized mining face is 20 mm
2	The subsidence of coal seam floor in the direction of advance of fully mechanized mining face is 40 mm
3	The subsidence of coal seam floor in the direction of advance of fully mechanized mining face is 60 mm

Table 6 Straightness error of the scraper conveyor with different floor sag

Test serial number	Fluctuation of coal seam floor (mm)	Straightness error (mm)		
		Maximum error	Minimum error	Average error
1	- 20	7.3	0.12	2.7
2	- 40	6.8	0.40	3.1
3	- 60	7.2	0.05	3.6
4	- 80	8.2	0.70	4.5
5	- 100	7.8	1.00	7.6

simulate the coal cutting process of shearer with scraper conveyor as running track, to study the influence of the undulations of coal floor on the straightness of scraper conveyor and the reliability of the motion law of floating connection mechanism.

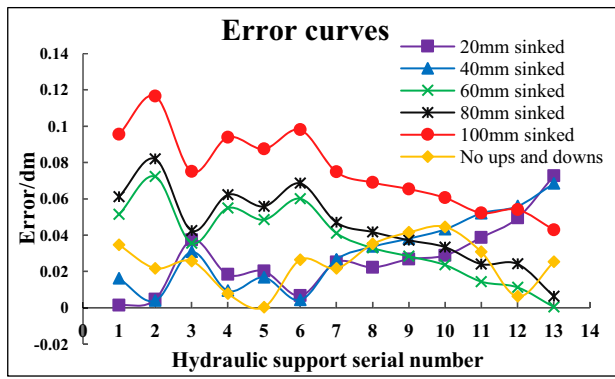
### 7.2 Experimental data analysis

Due to the large amount of data in this experiment, a portion relevant experimental data is selected as follows (Fig. 19).

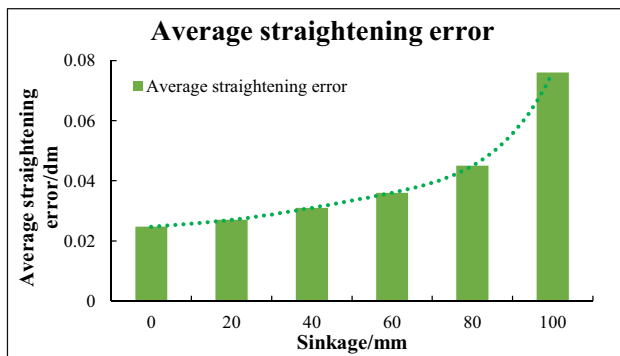
### 7.3 Reliability analysis of experimental device

Compare the data from the pushing test-bed with the data from the virtual simulation test, i.e., compare the data from the experiment with the data from Unity3D, and get the difference after the virtual-real comparison, to determine whether the test-bed can be used to verify the relevant conclusions from the virtual simulation test.

It can be seen from Fig. 20 that the difference between roll angle, pitch angle and yaw angle of the middle trough is within 1°, and the average value of difference of angle for middle groove is within 0.5° in Fig. 20d. This indicates that relevant tests are carried out on the pushing test-bed to validate the conclusions obtained in the virtual simulation test in this paper are feasible and effective.



(a) Error curves



(b) Average straightening error

Fig. 16 Straightening error of coal seam floor in the process of subsidence

### 7.4 Verification of motion law of floating connection mechanism

By comparing the experimental data with the data transported in the virtual environment, the D-value curves are obtained as shown in the Fig. 21.

As can be seen from Fig. 21, the average difference of the piston rod elongation is about 0.41 cm, and the average difference between the yaw angle of the push rod, the pitch angle and the yaw angle of the piston rod is about (0.45°, 0.10°, 0.09°), the difference between the experimental results and the virtual simulation results is small. This shows that the motion law of the floating connection mechanism obtained in this paper is true and reliable.

### 7.5 Verification of the influence of coal seam floor undulation on scraper conveyor straightness

#### 7.5.1 Straightening experiment in bulge topography

The coal floor model on one side of scraper conveyor is padded up to simulate the bulge topography by gaskets. The scraper conveyor is pushed by pushing mechanisms and the distance between the scraper conveyor and the location datum on the pushing mechanism is measured by displacement sensor. The straightness error curve of scraper conveyor under different bulge topography is obtained (Fig. 22).

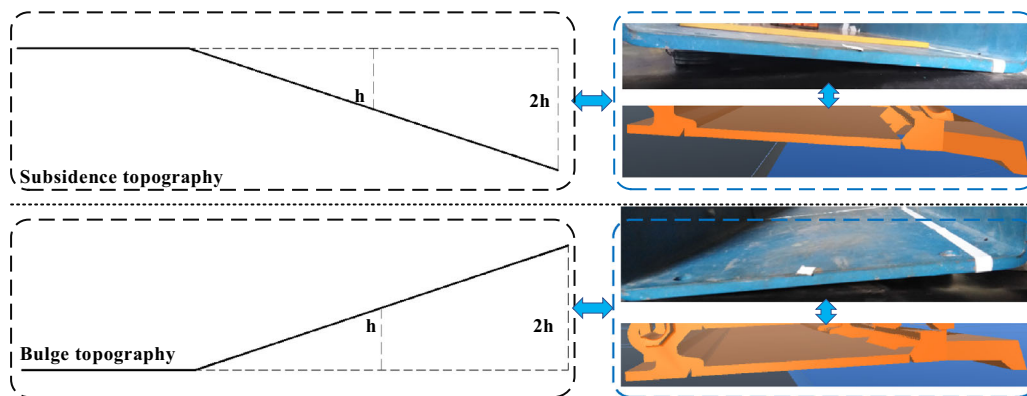


Fig. 17 Fluctuating model of coal seam floor

Table 7 The list of sensors

Sensor name	Sensor position	Role of sensors
MTi-300	The center of the board	To obtain the angle of the middle trough in real time
The tilt sensor	The relay bar	To obtain the angle of the relay bar in real time
The displacement sensor	The center of the middle trough	To obtain the distance between the center of the middle trough and the position datum of the push mechanism

It concludes that with the increase of coal seam floor undulation, the straightness error of scraper conveyor is increasing, and the average straightening error of the scraper conveyor increased flatly at first then steeply. The conclusions are consistent with the conclusions obtained in Sect. 6.1.

7.5.2 Straightening experiment in bulge topography

Raise the height of the coal seam floor by 5 gaskets as a whole, and the gaskets are placed under the bottom plate of one side of the scraper conveyor pushing an ear socket to simulate the subsidence topography. Repeat the experimental steps in Sect. 7.5.1 to get the straightness error curves of scraper conveyor under different subsidence, as shown in Fig. 23.

7.6 Experimental conclusions

- (1) The motion law of the floating connection mechanism obtained in this paper is correct.
- (2) The fluctuation of coal seam floor has influence on the straightness of scraper conveyor. It can be seen from Figs. 22a and 23a, when the coal seam floor fluctuates in the advancing direction of a fully mechanized coal mining face, the scraper conveyor straightness error increases after straightening. This conclusion verifies conclusion 2 in Sect. 6.3.
- (3) When the coal seam floor in the fully mechanized coal face has undulations, the straightness of scraper

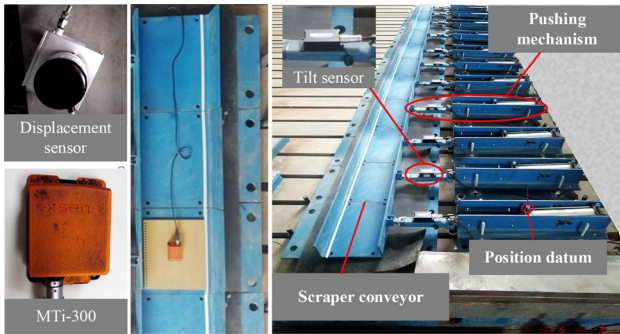
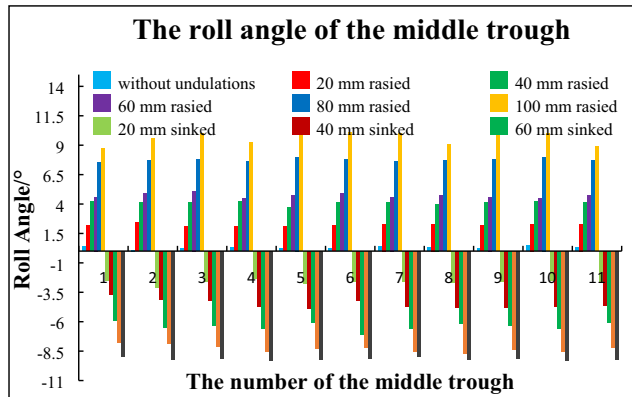
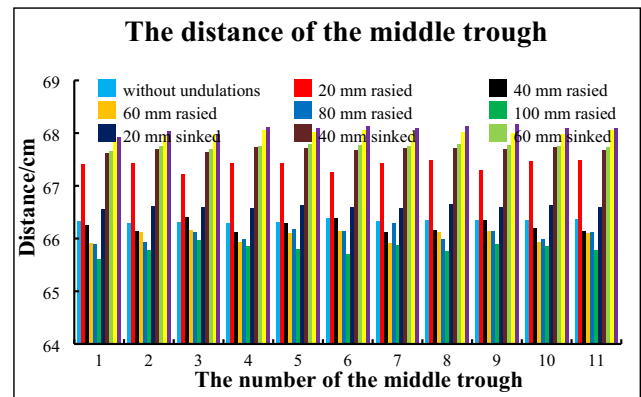


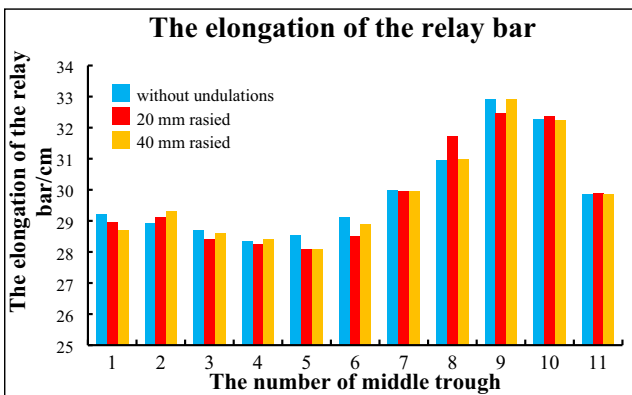
Fig. 18 Experimental equipment



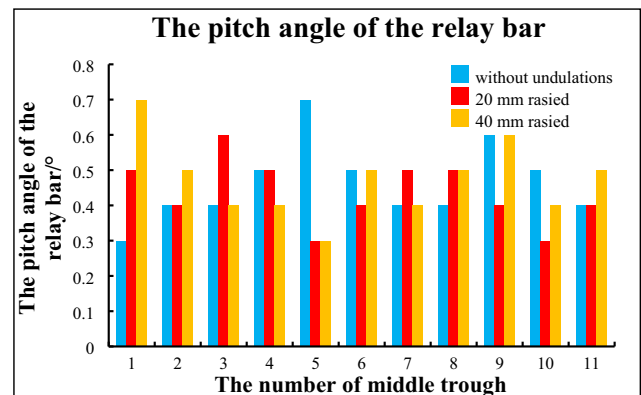
(a) The roll angle of the middle trough



(b) Distance of the middle trough from the position datum

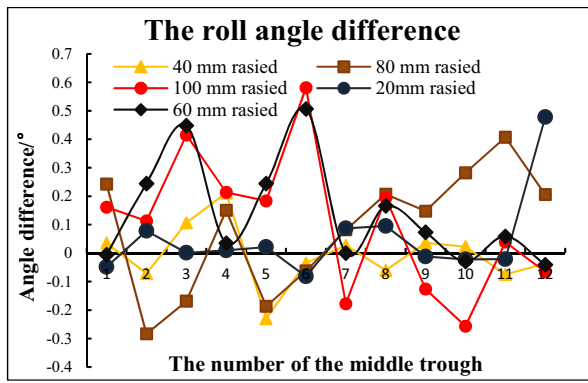


(c) The elongation of the relay bar

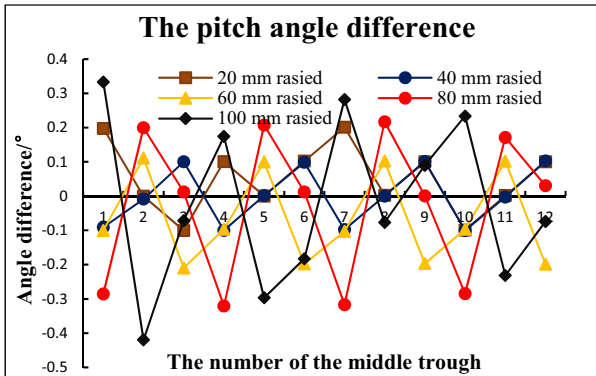


(d) The pitch angle of the relay bar

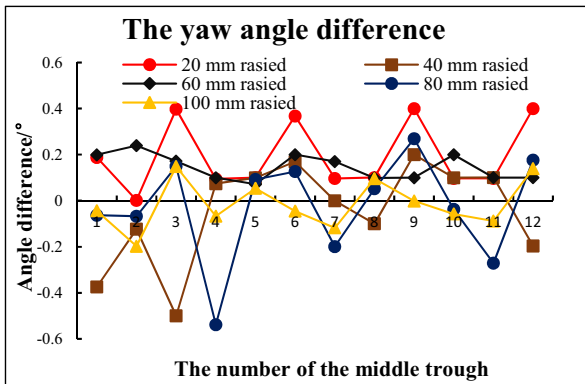
Fig. 19 Experimental data



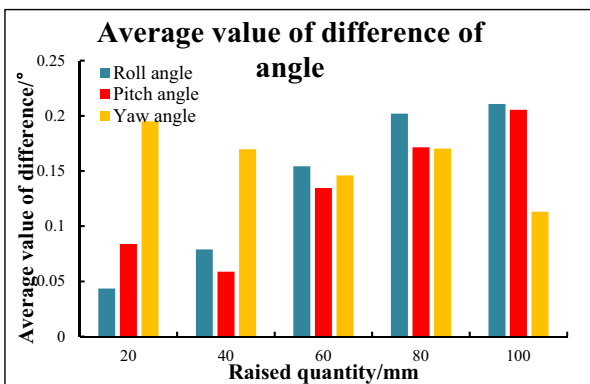
(a) Roll angle difference for the middle trough



(b) Pitch angle difference for the middle trough



(c) Yaw angle difference for the middle trough



(d) Average value of difference of angle

**Fig. 20** Virtual-real comparison of difference value of middle trough angle under bulge topography

conveyor is more affected by the subsidence terrain during straightening than by the bulge terrain, which can be seen from the comparison between Figs. 22b and 23b. This conclusion verifies conclusion 3 in Sect. 6.3.

Therefore, the conclusions of the influence of coal seam floor fluctuation on the straightness of scraper conveyor are correct, and they can indirectly show that the straightening method proposed in this paper is feasible.

## 8 Comparative analysis and simulation test

To verify the advantages of the straightening method described in this paper, the principle of LASC is used to straighten the floor of a complex cutting coal seam, and the straightening results are compared to the default straightening method in the established simulation system.

### 8.1 Comparison of straightening methods

LASC technology is a set of automatic mining technology, developed by the Commonwealth Scientific and Industrial Research Organization (CSIRO) (Ralston et al. 2015; Jonathon et al. 2017), adopts a strapdown inertial navigation system that can determine the coordinate position of a shearer in the three-dimensional space of a coal mine very accurately, monitor the three-dimensional attitude of a shearer in real time, and describe the walking track curve of a shearer through integrated navigation combined with the shearer’s odometer data (Ralston et al. 2015; Holm et al. 2013). In addition, the projection of the curve in the horizontal direction can be used in the process of automatic straightening of the working face (Li 2019).

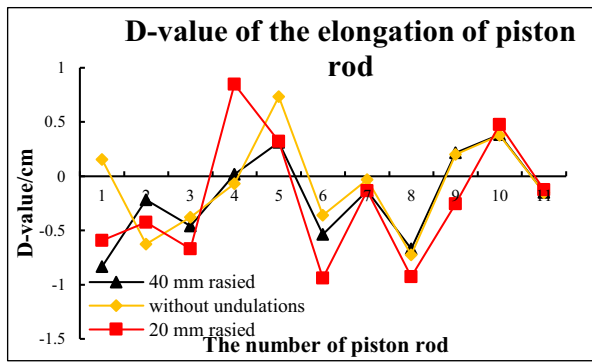
The LASC straightening technology is based on the LASC technology, the hydraulic support is advancing according to the difference between the predicted trajectory of the scraper conveyor and the current trajectory, and then the hydraulic support pushes the scraper conveyor at full stroke, so that the scraper conveyor can meet the requirements of straightness.

The differences between the LASC straightening principle and the proposed straightening method are shown in Table 8.

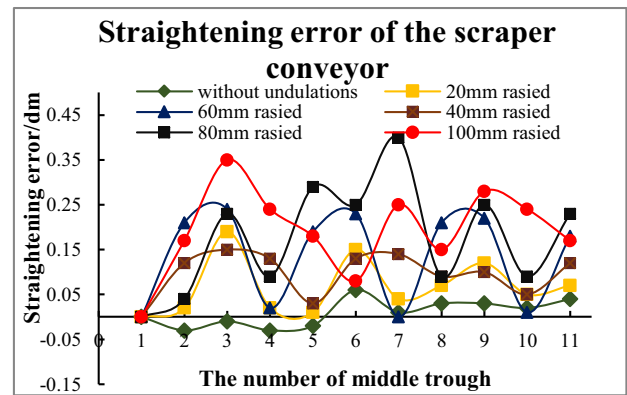
### 8.2 Comparison of simulation results

A simulation using LASC straightening was performed in order to compare LASC results to the results obtained by the proposed method.

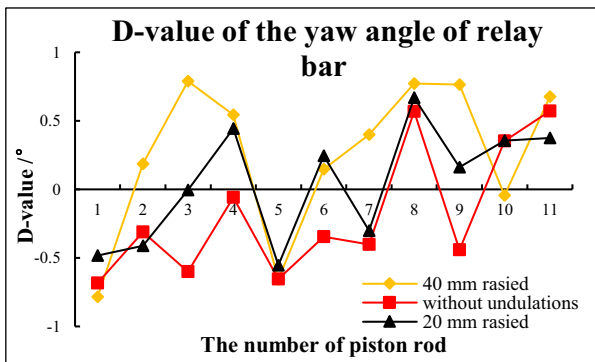
The straightening principle of the “Coal Seam + Equipment” Joint Virtual Straightening System is



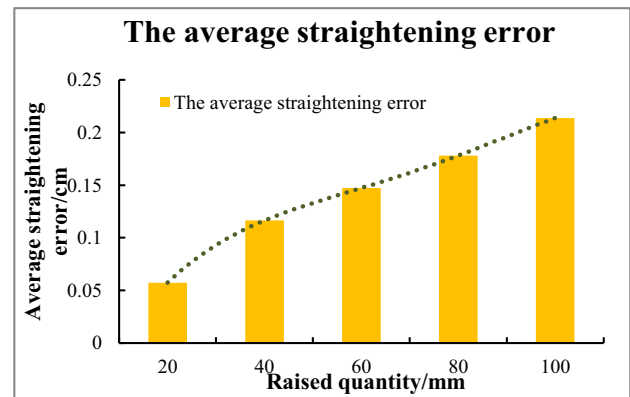
(a) D-value of the elongation of piston rod



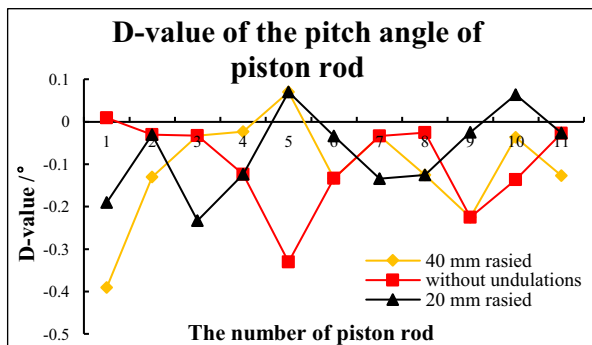
(a) Straightening error of the scraper conveyor



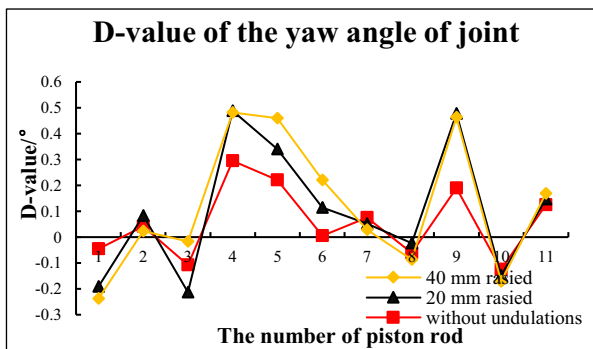
(b) D-value of the yaw angle of relay bar



(b) The average straightening error



(c) D-value of the pitch angle of piston rod



(d) D-value of the yaw angle of joint

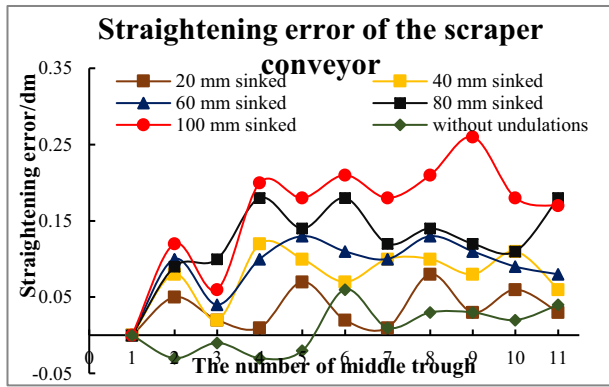
Fig. 21 D-value curves

Fig. 22 Error curves of scraper conveyor

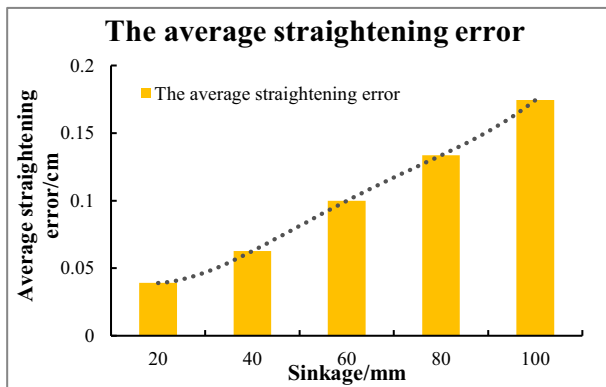
changed to the principle of LASC straightening. When the coal seam floor has no fluctuations in the running direction of a fully mechanized coal mining face, the scraper conveyor's straightening state and the fluctuation of the coal seam floor are consistent with the conditions described in Sect. 6 The straightening process is shown in Fig. 24. Figure 24a shows the initial state of the scraper conveyor, Fig. 24b shows the process of hydraulic support pushing the scraper conveyor, Fig. 24c shows the process of hydraulic support moving according to the straightening correction, and Fig. 24d shows the process of hydraulic support full stroke pushing scraper conveyor straightening.

The final position curve of each process of the horizontal projection of the scraper conveyor track is obtained, as shown in Fig. 25a, and, as can be seen, the straightening effect is better. It can be seen from Fig. 25b that, after straightening, the error between the actual track curve and the ideal track curve of the scraper conveyor is within  $-0.056$ – $0.078$  dm, and the straightening accuracy is relatively high.





(a) Straightening error of the scraper conveyor



(b) The average straightening error

Fig. 23 Error curves of scraper conveyor

As shown in Table 9, when the coal floor is no longer the ideal horizontal floor, after applying the principle of LASC, the average straightening error of the system is

larger than that of the default straightening method in the virtual environment.

The average straightening errors of the two straightening methods are compared in Fig. 26. In Fig. 26a, b, c, the difference between the average straightening error curve of LASC straightening technology and the proposed straightening method and the difference between them can be seen. The area above the abscissa is larger than the area below, which shows that overall the straightening error difference of the former is larger than that of the latter, and the difference is within 10 mm. In summary, the proposed straightening method has higher straightening accuracy than that using LASC straightening technology.

Due to the limitation of experimental conditions, it is impossible to verify the results of the comparative analysis simulation experiment. However, through the experimental results in Chapter 7, the comparative simulation test results in this chapter are also correct.

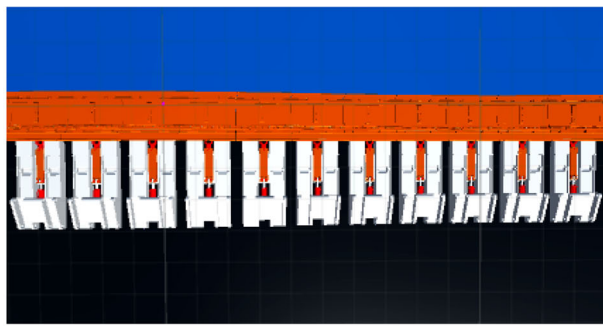
### 9 Conclusions and prospect

In this paper, the influence of the fluctuation of the coal seam floor on the straightness of a scraper conveyor has been investigated. First, the motion law of the floating connecting mechanism is obtained based on the pose solution of the industrial robot model, and a joint virtual straightening system of “Coal Seam + Equipment” is established. Through relevant simulation tests and comparative analysis, the following conclusions are obtained.

- (1) The precise push–pull movement of hydraulic support in a virtual environment is realized. In this paper, the motion law of the floating connecting mechanism is obtained based on the pose solution of

Table 8 Comparison of straightening methods

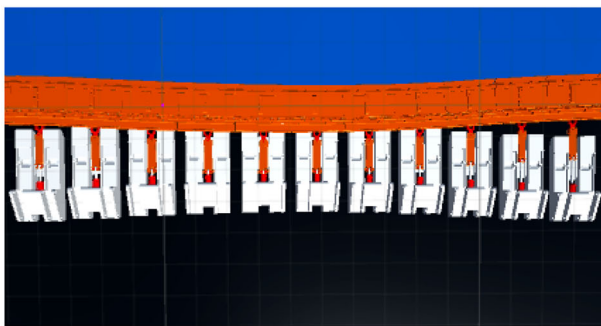
Straightening method	Principle	Differences
LASC straightening principle	Pushing → Advancing support according to the straightening correction amount → Pushing at full stroke	1. The former uses the straightening correction of Fig. 12, $RPC_n$ as the moving frame. In the latter, the actual elongation of the hydraulic cylinder corresponding to the $DPC_n$ in Fig. 12 is taken as the pushing stroke, and the elongation of the hydraulic cylinder corresponding to the $RPC_n$ straightening correction is taken as the advancing stroke
Straightening method based on motion law of floating connection mechanism	Pushing → Advancing support according to the elongation of the piston rod corresponding to the difference value $DPC_n$ → Pushing according to the elongation of the piston rod corresponding to the straightening correction value	2. The order of pushing and advancing of hydraulic support is different



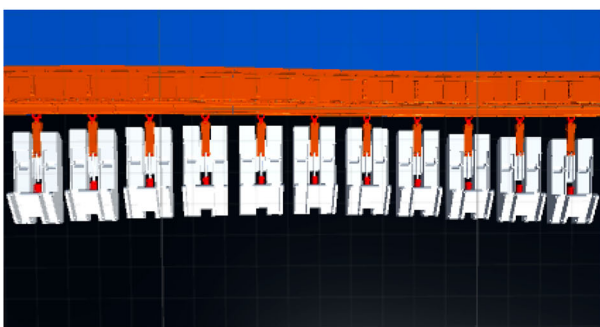
(a) Initial state



(b) Pushing

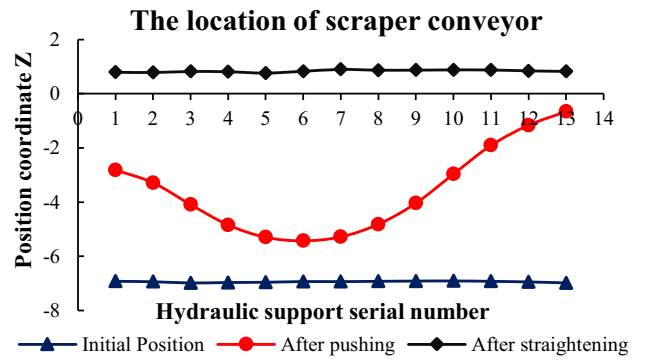


(c) Advancing support

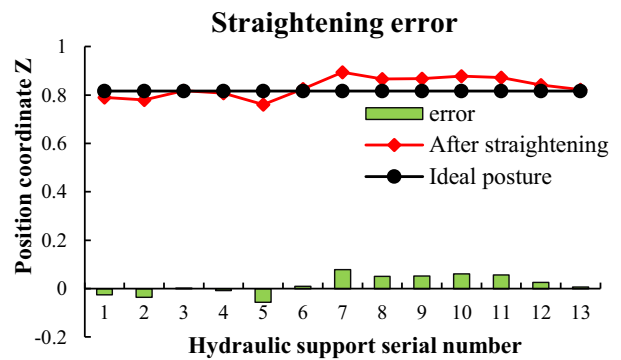


(d) Full stroke pushing

Fig. 24 Virtual straightening with LASC Technology



(a) The location of scraper conveyor



(b) Straightening error

Fig. 25 Location of scraper conveyor and straightening error

Table 9 Comparison of average straightening error

Fluctuation of coal seam floor (mm)	Average error (mm)		
	Adjustment method based on motion law of floating connection mechanism	Straightening method of LASC technology	Difference
0	2.5	3.7	0.8
20	3.81	10.1	6.29
-20	2.7	3.6	0.9

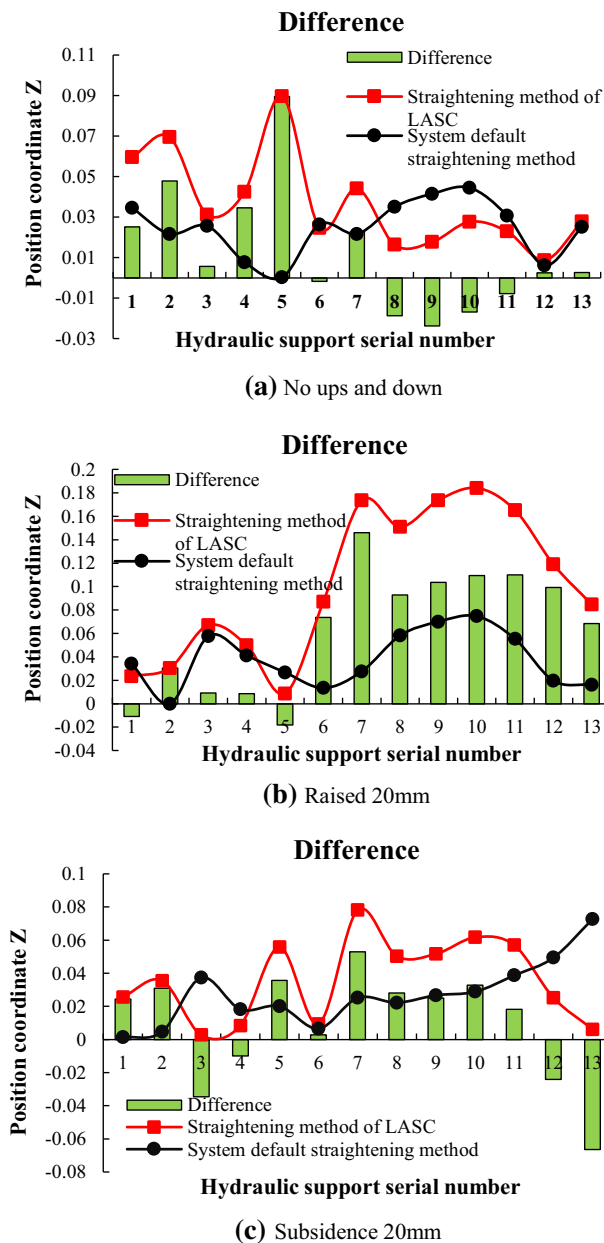


Fig. 26 Error comparison

the industrial robot model, which can be transformed into a form that can be used by the electro-hydraulic control system, which lays a foundation for the accurate movement in the physical environment.

- (2) The fluctuation of coal seam floor has a significant influence on the straightening accuracy of a scraper conveyor. The larger the fluctuation of the coal seam floor along the advancing direction of a fully mechanized coal mining face, the greater the straightness error. And the subsidence of coal seam

floor has a great influence on the straightening accuracy of scraper conveyor.

- (3) The straightening method based on the motion law of the floating connection mechanism has high straightening accuracy. The straightening method proposed in this paper has high straightening accuracy when there is a complex cutting floor in the coal mine. Compared with the same conditions when the scraper conveyor is straightened using the principle of LASC technology, the proposed straightening method has high accuracy.

In this study, because the fluctuation of the coal seam floor is not the only change along the coal seam trend, i.e., the entire floor is uneven, it is necessary to construct a coal seam floor model in the virtual environment that is based on data information obtained from the real detection. In addition, this paper only considers the undulation of the coal seam floor in the advancing direction of the fully mechanized coal face and the existence of the coal seam dip angle. Faults, folds, and other complex geological structures complicate the advancing and straightening process of the fully mechanized coal face.

In future research, the above conclusions should be verified in combination with the actual coal mining process, and the influence of the complex coal seam floor on the straightening of the fully mechanized mining face should be further studied. According to geological structure models, such as faults and folds, the virtual floor model is established to explore the cooperation between hydraulic support and scraper conveyor under the complex geological structure in order to lay the foundation for the establishment of a fully mechanized mining face production system based on digital twin and to promote the construction of an “Intelligent Mine”.

**Acknowledgements** This research was supported by the Project funded by National Natural Science Foundation of China (Grant No. 52004174), China Postdoctoral Science Foundation (No. 2019M651081), the Key Research and Development Program of Shanxi (201903D121141), the Natural Science Foundation of Shanxi Province (201901D211022), the Scientific and Technological Innovation Programs of Higher Education Institutions in Shan Xi (No. 2019L0305).

**Author contributions** Suhua Li studied and designed the theoretical part and the experimental part respectively; Jiacheng Xie reviewed the theoretical part and the experiment; Fang Ren and Xin Zhang performed the experiments; Xuwen Wang and Binbin Wang contributed materials/analysis tools; Suhua Li wrote the paper.

**Compliance with ethical standards**

**Conflict of interest** The authors declare no conflict of interest.

**Open Access** This article is licensed under a Creative Commons Attribution 4.0 International License, which permits use, sharing,

adaptation, distribution and reproduction in any medium or format, as long as you give appropriate credit to the original author(s) and the source, provide a link to the Creative Commons licence, and indicate if changes were made. The images or other third party material in this article are included in the article's Creative Commons licence, unless indicated otherwise in a credit line to the material. If material is not included in the article's Creative Commons licence and your intended use is not permitted by statutory regulation or exceeds the permitted use, you will need to obtain permission directly from the copyright holder. To view a copy of this licence, visit <http://creativecommons.org/licenses/by/4.0/>.

## References

- Chen Y, Dong F (2013) Robot machining: recent development and future research issues. *Int J Adv Manuf Technol* 66(9–12):1489–1497
- Fan Q, Li W, Luo C (2012) Error analysis and reduction for shearer positioning using the strapdown inertial navigation system. *Int J Comput Sci* 9(5):49–54
- Fang XQ, Zhao J, Hu Y (2010) Tests and error analysis of a self-positioning shearer operating at a manless working face. *Min Sci Technol* 20(1):53–58
- Fang X, Ning Y, Li S et al (2019) Research on key technique of straightness perception of scraper conveyor based on fiber grating. *Coal Sci Technol* 47(1):152–158
- Fu RK, Zhang CY, Zhang H (2017) Discovery and outlook on intelligent sensing and control technology of mine fully-mechanized mining. *Coal Sci Technol* 45(9):72–78
- Ge S, Hao S, Zhang S et al (2020) Status of intelligent coal mining technology and potential key technologies in China. *Coal Sci Technol* 48(7):28–46
- Hao SQ, Wang SB, Malekian R et al (2017a) A geometry surveying model and instrument of a scraper conveyor in unmanned longwall mining faces. *IEEE Access* 5:4095–4103
- Hao S, Wang S, Malekian R et al (2017b) A geometry surveying model and instrument of a scraper conveyor in unmanned longwall mining faces. *IEEE Access* 5:4095–4103
- Holm M, Beitzler S, Arndt T et al (2013) Concept of shield-data-based horizon control for longwall coal mining automation. *IFAC Proc* 46(16):98–103
- Ibrahim AH, Claus GS, Dionysis B et al (2011) Field robotics in sports: automatic generation of guidance lines for automatic grass cutting, striping and pitch marking of football playing fields. *Int J Adv Robot Syst* 8(1):113–121
- Isleyen E, Duzgun HS (2019) Use of virtual reality in underground roof fall hazard assessment and risk mitigation. *Int J Min Sci Technol* 29(4):603–607
- Jazar RN (2010) *Theory of applied robotics: kinematics, dynamics, and control*. Springer, Berlin
- Jonathon CR, Chad OH, Mark TD (2017) Longwall automation: trends, challenges and opportunities. *Int J Min Sci Technol* 27(5):733–739
- Li S (2019) Measurement & control and localisation for fully-mechanized working face alignment based on inertial navigation. *Coal Sci Technol* 47(8):169–174
- Li A, Hao SQ, Wang SB et al (2016) Experimental study on shearer positioning method based on SINS and Encoder. *Coal Sci Technol* 44(4):95–100
- Liu T, Tan C, Wang Z et al (2019) Horizontal bending angle optimization method for scraper conveyor based on improved bat algorithm. *Algorithms* 12(4):84
- Manou E, Vosniakos G-C, Matsas E (2019) Understanding industrial robot programming by aid of a virtual reality environment. *Int J Mech Eng Educ* 47(2):135–155
- Meng X, Li M, Sun J et al (2020) Complete sets of equipment and key technologies for intelligent fully-mechanized mining of ten-million tonnage level mine. *Coal Sci Technol* 48(7):47–54
- Niu JF (2015) Study on automatic and intelligent following control system of hydraulic powered support in fully-mechanized coal mining face. *Coal Sci Technol* 43(12):85–91
- Ralston JC, Reid DC, Dunn MT, Hainsworth DW (2015) Longwall automation: delivering enabling technology to achieve safer and more productive underground mining. *Int J Min Sci Technol* 25(06):865–876
- Reid DC, Hainsworth DW, Ralston JC et al. (2011) Inertial navigation: enabling technology for longwall mining automation. In: European Commission, Luxembourg, pp 1–14
- Shi HB, Xie JC, Wang XW et al (2019) An operation optimization method of a fully mechanized coal mining face based on semi-physical virtual simulation. *Int J Coal Sci Technol* 7:1–17
- Syd SP, Feng D, Jingyi C, Yang L (2019) Automation in U.S. longwall coal mining: a state-of-the-art review. *Int J Min Sci Technol* 29(02):151–159
- Wang JH (2014) Development and prospect on fully mechanized mining in Chinese coal mines. *Int J Coal Sci Technol* 1(3):253–260
- Wang JH, Huang ZH (2017) The recent technological development of intelligent mining in China. *Engineering* 3(04):24–35
- Wang SB, Zhang BY, Wang SJ et al (2018) Dynamic precise positioning method of shearer based on closing path optimal estimation model. *IEEE Trans Autom Sci Eng* 16:1–8
- Wang GF, Liu F, Pang YH et al (2019) Coal mine intellectualization: the core technology of high quality development. *J China Coal Soc* 44(2):349–357
- Wang J, Song S, Li P (2020) An experimental research of dynamic characteristics for long wall shearer cutting unit gearbox in oblique cutting. *Int J Coal Sci Technol* 7:388–396. <https://doi.org/10.1007/s40789-020-00296-2>
- Wu M (2013) Comparative study on CBM development program for deep tectonic coal within mining area, Xin'an coalmine. China University of Geosciences, WuHan
- Xie JC (2018c) Method of monitoring and dynamic planning for three machines in a fully mechanized coal-mining face under VR environment. Dissertation, Taiyuan University of Technology
- Xie JC, Yang ZJ, Wang XW et al (2017) A joint positioning and attitude solving method for shearer and scraper conveyor under complex conditions. *Math Probl Eng* 2017:1–14
- Xie JC, Yang ZJ, Wang XW et al (2018a) Cooperative solving method of chute postures in the bending section of a scraper conveyor. *Adv Mech Eng* 10(3):1–13
- Xie JC, Yang ZJ, Wang XW et al (2018b) A virtual reality collaborative planning simulator and its method for three machines in a fully mechanized coal mining face. *Arab J Sci Eng* 43(9):4835–4854
- Xie JC, Yang ZJ, Wang XW et al (2018) A remote VR operation system for a fully mechanized coal-mining face using real-time data and collaborative network technology. *Min Technol* 127:1–11
- Xie JC, Wang XW, Yang ZJ et al (2019) Virtual monitoring method for hydraulic supports based on digital twin theory. *Min Technol* 128:1–11
- Zhang Q, Wang Y, Wang H et al (2019) Electromechanical coupling model and dynamics simulation analysis of two-motor drive scraper conveyor. *Coal Sci Technol* 47(1):159–165